NUISANCE FLOODING IN HONOLULU, HI:
A CASE STUDY OF SUMMER 2017

A THESIS SUBMITTED TO
THE GLOBAL ENVIRONMENTAL SCIENCE
UNDERGRADUATE DIVISION IN PARTIAL FULFILLMENT
OF THE REQUIREMENTS FOR THE DEGREE OF

BACHELOR OF SCIENCE

IN

GLOBAL ENVIRONMENTAL SCIENCE

AUGUST 2018

By
Ashley Hi‘ilani Sanchez

Thesis Advisor

Philip Thompson, PhD

I certify that I have read this thesis and that, in my opinion, it is satisfactory in scope and quality as a thesis for the degree of Bachelor of Science in Global Environmental Science.

THESIS ADVISOR

Philip Thompson, PhD
Department of Oceanography

For my grandpa, who loved the ocean.

Taylor Kuumealoha Kaʻaina
March 14, 1935 – January 17, 2018

Acknowledgements

I wish to thank the following people and agencies for their advice and support during this project and my matriculation in the GES program:

Dr. Phil Thompson

Dr. Eric Firing

Dr. Brian Powell

Dr. Michael Guidry

The University of Hawai‘i Sea Level Center

The Hawai‘i and Pacific Islands King Tides Project

Abstract

The summer of 2017 broke sea level records and had an unprecedented number of nuisance flooding events. The King Tides Project provided a photo database of nuisance flooding events in Mapunapuna. Multiple contributions to sea level were observed during these events, including Rossby waves, eddies, the inverted-barometer effect, and tides. High tides were found to be the primary indicator of when a nuisance flooding event may have occurred, although this was not always the case. The results from this study can be applied to the King Tides database to expand the information on these events by corroborating their photographic metadata with physical quantifications.

Table of Contents

List of Tables

List of Figures

Preface

The Intergovernmental Panel on Climate Change (IPCC) predicts global average sea level to rise by as much as one meter by the year 2100 due to melting of ice in polar regions and thermal expansion of water caused by increased global temperatures associated with anthropogenic climate change (Church et al., 2013). The direct impacts of this sea level rise will be experienced along all coastlines, but the consequences will be especially severe for low-lying islands and atolls. Island communities are vulnerable to open ocean swell and are situated over shallow terrestrial water tables. Increasing sea level causes wave runup to reach further inland and the water table to rise closer to the surface, causing inland flooding.

The State of Hawai‘i is particularly vulnerable to sea level rise due to the importance of the state’s coastline to its economy and culture, and the impacts will transcend socioeconomic boundaries. Tourism is listed as the state’s greatest economic driver (Department of Business Economic Development & Tourism, n.d.). Beaches are the dominant contributor to the appeal of Hawai‘i as a tourist destination, but this asset is threatened by rising seas. For example, the total erosion of Waikīkī Beach would be expected to cost the state $2 billion in tourist expenditures alone, considering that 42% of all tourism revenue originates in the Waikīkī area (Cocke, 2015). With no sand on the beach, tourists would have little reason to visit, putting surrounding Waikīkī businesses in jeopardy. Even the beachfront property itself, which is coveted real estate throughout Hawai‘i, would decrease in value and impact the finances of local residents and off-island investors.

National defense is another crucial component of the Hawaiian economy that is threatened by sea level rise (Department of Business Economic Development & Tourism, n.d.). All branches of the U.S. armed forces—Army, Navy, Marines, Coast Guard, and Air Force—maintain bases in Hawai‘i, providing military families and local residents alike with jobs. These federal positions make up over 12% of all employment in the state. They bring work otherwise unavailable to the islands and stimulate the economy (Department of Business Economic Development & Tourism, n.d.). Many of these bases, such as Joint Base Pearl Harbor-Hickam in Honolulu and the Kāne‘ohe Bay Marine Corps Base, are located in coastal regions on O‘ahu. Therefore, sea level rise has the potential to cause damage to federal property and may force adaptation or relocation, causing substantial financial loss to the local economy.

The economy is not the only component of life in Hawai‘i at risk due to sea level rise. The unique Native Hawaiian culture is active and prominent throughout Hawai‘i. A tenet of this culture is to have a humble and respectful communion with the surrounding land and ocean. Thus, sea level rise threatens more than dollars; it threatens a way of life for Hawaiians and long-term residents alike. Throughout the islands, sacred areas, monuments, and structures that are cherished and revered by the Hawaiian people are currently at risk of being degraded or destroyed by the effects of sea level rise. In addition, Hawaiian people have an intimate relationship with the islands’ ecosystems, and sea level rise threatens traditional aquaculture practices, such as saltwater fish ponds, as well as essential habitat for marine species such as sand crabs, green sea turtles, and the endangered Hawaiian monk seal.

In total, the pervasive nature of stresses that sea level rise places on Hawaiian society demands action from local and federal legislation. For the urban Honolulu area alone, it is projected that a significant number of roads and infrastructures, 80% of the economy, and nearly half of the population are currently at risk of inundation from sea level rise (Hawai‘i Climate Change Mitigation and Adaptation Commission, 2017). However, many decision makers are not aware that slow, long-term sea level rise is not the only factor involved in consideration of sea level impacts. Hawai‘i experiences sea level fluctuations on a variety of time scales ranging from daily to decadal, and these shorter-term fluctuations can cause the impact of climate change to be experienced much sooner than expected from the long-term trend alone.

The best example of the impact of these non-secular fluctuations in sea level is the record-setting summer of 2017 during which the island of O‘ahu experienced an unprecedented number of minor flooding events. Nuisance flooding, otherwise known as high tide flooding, is flooding which causes inconvenience to the public such as inaccessibility to homes or businesses and road closures (Figure 1, NOAA, 2018). When sea level anomalies, such as anticyclonic eddies, ocean swells, and the transition from El Niño conditions, coincide with normal seasonal high tides, the effects of all the phenomena are ‘stacked’ creating an extreme sea level event that can cause nuisance flooding (Virtue, 2017). This was just the case in Hawai‘i during the summer of 2017 when the observed sea level broke the 112-year Honolulu tide gauge record (Virtue, 2017). Honolulu is vulnerable to the effects of nuisance flooding because of the city’s low elevation and proximity to the ocean. It is understandable that Honolulu coastal areas like Waikīkī are influenced by high sea level events by nature of their proximity to the ocean; however, the influences of sea

level on low-lying inland areas like the business district of Mapunapuna are less obvious. The impacts of extreme variation to sea level became apparent in Mapunapuna during the summer of 2017 when flooding occurred. As visible in Figure 2, favorable weather conditions were present at the time, so flooding attributed to rainfall had no likely contribution.

In this thesis, I will use the summer of 2017 as a case study to document the relative importance of all contributions to sea level extremes in Hawai‘i. To do this, I will quantify observational tide gauge and satellite altimetry data, perform various analyses on these data to produce results attributable to sea level extremes, and draw meaningful conclusions based on the results. One of my goals is to apply the physical data and analyses found herein to the Hawai‘i and Pacific Islands King Tides Project photo database in order to improve the understanding of sea level in Honolulu and provide insight to future conditions.

Figure 1. Nuisance/High Tide Flooding (adapted from NOAA, 2018)

Figure 2. Nuisance flooding in the inland Honolulu business district of Mapunapuna during a sea level extreme in Summer 2017 (Photo: Dolan Eversole of Hawaii Sea Grant)

Chapter 1. Introduction

1.1 What is sea level?

There are many direct and indirect physical forcings that contribute to sea level change on multiple time scales, but before describing these various contributions in Hawai‘i, it is important to clearly define what ‘sea level’ means. Sea level is, of course, a measurement of the height of the ocean surface as it rises and falls, but how do we measure it? Sea level is the height relative to what? Choosing a baseline with which to measure sea level by depends on what is being studied. *Absolute,* or *eustatic*, sea level is a measurement of the height of the ocean with the center of the Earth as a baseline reference. It assumes Earth is a static mass and there is no account for changes to uplifting or subsidence of land. In contrast, *relative* sea level measures the changes to the height of the ocean relative to a fixed point on land. If we are concerned with the impacts of sea level rise, we are concerned with relative sea level, since it is change relative to land that will affect coastal areas like those found throughout the Hawaiian Islands.

1.2 Contributions to relative sea level variability in Hawai‘i

1.2.1 Sea level change on geologic time scales

Throughout Earth’s history, sea level has varied by 4-6 m above present during the last warm period (125,000 years ago) to 120 m below present during the last cold period (20,000 years ago; Gornitz, 2012). The largest prehistoric sea level changes occurred on geologic time scales and were onset by astronomical phenomena, called Milankovitch cycles, which describe Earth’s astronomical orientation around the Sun (Hays et al., 1976). Eccentricity, or the shape of the elliptical orbit Earth follows around the Sun, changes between high and low obliquity approximately every 100,000 years. The tilt of the center

axis of Earth changes the degree of tilt with a periodicity of 41,000 years. Procession of the equinoxes changes the direction of the central axis of Earth—much like a wobbling top—and occurs with a periodicity of 23,000 years. Depending on the orientation of Earth toward the Sun, the combination of these Milankovitch cycles may either push Earth into a cold glacial period, or ice age, where much of the surface of Earth is covered by ice, or it may push Earth out of a glacial period and into a warm interglacial period where glacial regions rapidly melt and ice only covers the polar regions, similar to the climate we are experiencing today (Hays et al., 1976). The enormous meltwater pulses during the transition into an interglacial period can cause sea level to change 10 mm/year on average, even rising as quickly as 26-53 mm/year (Gornitz, 2012). As Earth finished the most recent transition from a glacial to an interglacial period, most melting ceased about 6,000 years ago, and the rate of sea level rise over the past 2,000 years has remained low, averaging 0.0-0.2 mm/year (Church et al., 2013; Gornitz, 2012). The increasing sea levels we are currently experiencing do not coincide with any of the aforementioned phenomena which could onset sea level rise and is thus an unprecedented trend in Earth's geologic history.

1.2.2 Historical and recent global mean sea level rise

The most significant concern with current estimates and projections of sea level is that there is an unprecedented pattern of rising mean relative sea level measurements across the globe. With 95% certainty, this trend is attributed to anthropogenic inputs of carbon dioxide into the atmosphere caused by burning fossil fuels (Church et al., 2013). Carbon dioxide is considered a greenhouse gas and acts as an insulator, trapping incoming longwave solar radiation, thereby causing an increase to the temperature at the surface of the Earth known as the "greenhouse effect." This heating leads to the melting of ice in polar

regions, such as Greenland and Antarctica. The input of meltwater from these ice sheets raises mean eustatic sea level and is the main contributor to sea level rise. Another significant component to sea level rise is the thermal expansion of water itself. With increasing temperatures, water decreases in density and expands due to its thermal properties.

As estimated from tide gauge data, the global mean rate of sea level rise during the 20th century is given by the IPCC as 1.8 mm/year; however, the measurements taken by the TOPEX/Poseidon and Jason satellites have observed global mean sea level rise at the rate of 3.3 mm/ year. The change to sea level over the entire altimetry period (1992-2015) has been an overall increase of 70 mm (Nerem & National Center for Atmospheric Research Staff (Eds), 2016). A recent study has shown the rate of ice melt over the altimetry period is accelerating faster than anticipated, and because of this, sea level may achieve a height twice that of current projections (Nerem et al., 2018). It is important to note that there are discrepancies between the altimetry and tide gauge data because the length of the altimetry period is quite short (23 years) compared to the tide gauge record (+100 years); long-term conclusions cannot be drawn from the satellite altimetry alone.

Honolulu sea level has been shown to be steadily increasing at a mean rate of 1.4 mm/year since the tide gauge record began in 1905 (Figure 3). While slightly less than the global rate, the long-term trend in Honolulu is largely a manifestation of global mean sea level rise. The difference between the rate in Honolulu and the global rate can be attributed to modes of decadal climate variability which affect sea level (Firing & Merrifield, 2004).

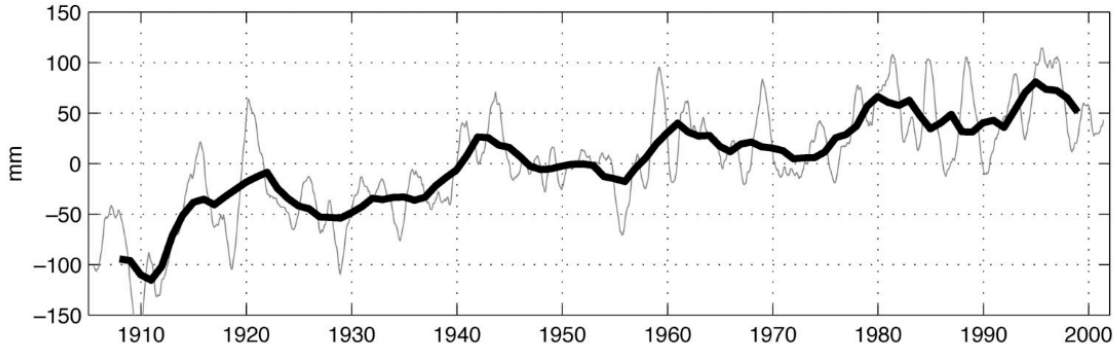

Figure 3. Honolulu sea level referenced to an arbitrary benchmark on land. The thin line shows annual means, and the thick line shows 5-yr means (Firing et al., 2005)

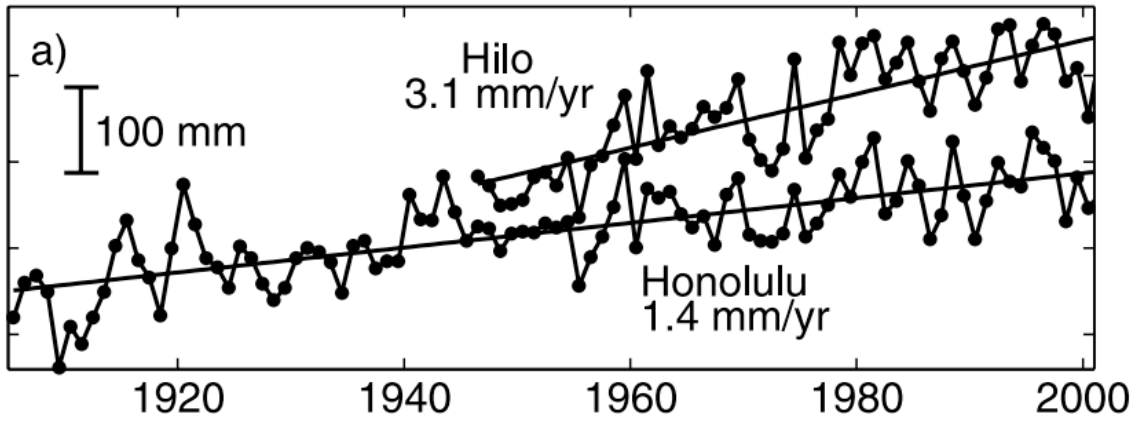

Figure 4. Annual mean sea level from Honolulu and Hilo (Caccamise et al., 2005)

1.2.3 Differences in long-term trends within the Hawaiian Islands

Caccamise et al. (2005) investigated the difference in the rate of sea level rise between Hilo, Hawai‘i and Honolulu, Hawai‘i. Hawai‘i Island outpaces O‘ahu with a rate +1.8 ± 0.4 mm/year (Figure 4). The difference in these rates was originally attributed to the contribution of the lithospheric subsidence of Hawai‘i Island, but the authors determined that thermal expansion of sea water was an important contributor to sea level in Hawai‘i. They found that lithospheric subsidence was not as influential on the difference

in sea level rates at Honolulu and Hilo as previously assumed, and that thermal expansion played a more significant role than expected in explaining the difference. The steric sea level contributed sometimes as much as half of the sea level rate difference between Honolulu and Hilo.

1.2.4 Decadal sea level variability

Sea level in Hawai‘i responds to basin-scale modes of decadal climate variability in the Pacific, such as the Pacific-North America index (PNA, Wallace & Gutzler, 1981) and the Pacific Decadal Oscillation (PDO, Mantua et al., 1997). The Southern Oscillation index, which represents the interannual and decadal signal of the El Niño Southern Oscillation, does not have a strong correlation to Hawai‘i sea level; however, the PNA was well correlated with interdecadal sea level at Hawai‘i, indicating an indirect relationship to tropical variability (Firing et al., 2005). Others have also confirmed a correlation with modes of interdecadal climate variability (Caccamise et al., 2005; Merrifield et al., 2012; Thompson et al., 2014). The PDO is associated with multiple modes of ocean variability, and fluxuates between warm and cool phases on inter-annual to inter-decadal time scales (Merrifield et al., 2012). The PNA index contains a significant interdecadal component, and is associated with fluctuations in sea level of 3-4 cm (Firing et al., 2005). Modes of interdecadal oscillations have been shown to be statistically correlated with sea level fluctuations and are caused by the wind field and westward propagation (Firing et al., 2005). When the Aleutian Low is stronger, the North Pacific High is weaker, corresponding to higher sea levels in Hawai‘i; a weaker Aleutian Low corresponds to a stronger North Pacific high and lower sea levels in Hawai‘i (Figure 5. Hawaii sea level (left) high and (right) low: (top) winter wind stress and sea level pressure, (middle) winter wind stress

anomaly and wind stress curl anomaly, and (bottom) sea surface height (Firing et al., 2005).).

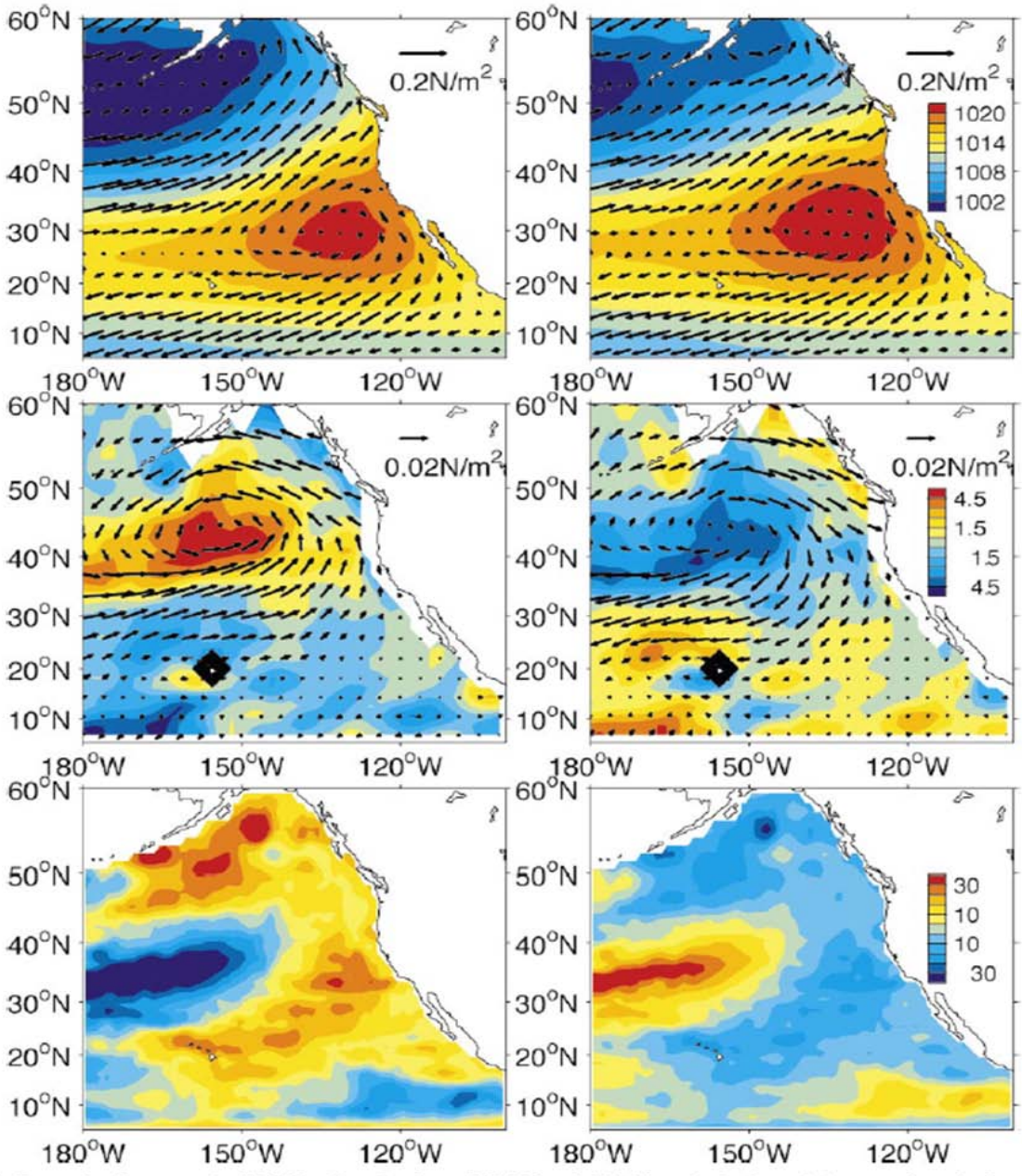

Figure 5. Hawaii sea level (left) high and (right) low: (top) winter wind stress and sea level pressure, (middle) winter wind stress anomaly and wind stress curl anomaly, and (bottom) sea surface height (Firing et al., 2005).

1.2.5 Planetary scale Rossby waves

Rossby waves are a type of internal wave made possible by the rotation of Earth and the curvature of the Earth. These waves were difficult to observe except at a few controlled stations and there was no evidence of their basin-wide resonance until only recently when adequate observations were made available by the advent of satellite altimetry (Chelton & Schlax, 1996). First baroclinic mode Rossby waves (second to the lowest order) propagate westward very slowly, at around 100 cm s^{-1} varying by latitude, and their amplitudes at the surface, or their contribution to sea level, are generally <10 cm (Chelton & Schlax, 1996). The time it takes for these waves to cross an entire ocean basin can range from months to decades.

1.2.6 Mesoscale eddies

Eddies are a commonplace feature in the North Pacific formed under baroclinic instability and the Earth's rotation. They are cyclonic or anticyclonic rotating parcels of water often generated by meanders of open ocean currents, currents emerging into the open ocean, or around physical barriers such as islands like Oʻahu and Hawaiʻi Island. Typical horizontal scales are between 10 and 100 km, and one full rotation typically takes 10-30 days. Eddies can persist in the ocean on scales from weeks to months. Regardless of origin, eddies are able to propagate parcels of water from their generation site to places elsewhere in the ocean, carrying retained heat or nutrients along. Cold core eddies are cyclonic in flow and are associated with a slight depression at the sea surface. Warm core eddies are anticyclonic and create a slight bulge of water at the sea surface. The characteristics of eddies make them a highlighted component of relative sea level. Examples of the magnitudes of eddy depressions and bulges shall be discussed in this study.

According to Firing & Merrifield (2004), “mesoscale eddies are a major contributor to short-term sea level variability in Hawaiian waters.” Eddies are prevalent around the Hawaiian archipelago due to complex flow/atmospheric variability but are particularly encouraged to form in the lee of Hawai‘i Island by prevailing northeasterly trade winds and island topography (Lumpkin & Flament, 2001; Yoshida et al., 2010). These eddies tend to propagate westward away from the archipelago but can also propagate along the ridge, impacting islands along the way.

1.2.7 Ice melt fingerprints

The mass of an ice sheet is great enough to exert a gravitational pull on the water surrounding it. This causes the sea surface height to increase in the vicinity of the ice sheet. There is also a deformation of the solid surface caused by the mass of the ice sheet and the resultant piling up of water. When an ice sheet melts, several feedbacks occur: the mass of the ice sheet decreases, which partially relaxes the gravitational pull holding the sea surface height near the ice sheet, and water is distributed away from the ice sheet, raising sea level elsewhere. With less ice and water mass above, the solid surface below responds by uplifting, thereby lowering relative sea level in proximity to the ice shelf. The particular spatial pattern of sea level change associated with these processes is called the ‘fingerprint’ of the melt source (Church et al., 2010).

The implication of melt fingerprints is that not every melt source has an equal effect on any given location. The fingerprint for the West Antarctic Ice Sheet (WAIS) is particularly severe for Hawai‘i, especially given the possibility for rapid ice mass loss from the WAIS over the remainder of the century. In the extreme case of 2 meters of global

mean SLR due to melt from West Antarctica, this will express in Hawai‘i as 2.8 meters of SLR—or 40% more than the global average (DeConto & Pollard, 2016).

1.2.8 Inverted-barometer effect

When low pressure atmospheric systems move over a body of water, the local sea level increases in order to preserve hydrostatic balance at the sea surface. High pressure systems result in a local decrease in sea level. Sea level pressure (SLP) is a measurement of the sea level contribution due to atmospheric pressure. It is considered a minor contributor to sea level, which will be confirmed in this study. The data are provided by NOAA’s Earth System Research Lab (ESRL) Physical Sciences Division (PSD). The measurements of SLP are in millibars. 1 mb of SLP increase corresponds to 1 cm of sea level decrease and vice versa. Using this relationship, the contribution to sea level caused by changes in the atmosphere can be determined.

1.2.9 Tides

Tides are defined as the rise and fall of sea level due to the gravitational effects of celestial bodies—mainly the Sun and the Moon—on Earth’s oceans. The most influential secular body is the Moon because of its proximity to Earth. During the full and new moons, Earth experiences higher high tides and lower low tides, known as *spring tides*. Conversely, during the first and third quarter moons, Earth experiences *neap tides,* or lower high tides and higher low tides. Tides vary the sea level in Honolulu by an average of approximately 0.6 m daily between high and low tides. Because of their astronomical origin, tides are a predictable ocean phenomenon and change with variations to Sun, Earth, and Moon geometry on time scales ranging from interdecadal to millennial. Different points throughout the 18.6 year lunar nodal cycle affect tidal variability in Hawai‘i (Haigh et al.,

2011). The impact of dynamic influences on sea level discussed above will be greatest during the highest tides of the year, which occur during summer and winter months in O‘.

1.3 Extremes and Flooding

In the IPCC’s Fifth Assessment Report (AR5), the authors have shown statistical evidence of an increase in observed sea level extremes caused primarily by the processes discussed in Section 1.2. These processes occur on different spatial and temporal scales, but when they have positive values of sea level contribution that coincide with one another, their effects are additive and may cause a sea level extreme, which may then lead to a flood event. There is evidence that regions around the US are already experiencing increases in minor coastal flooding events (Sweet et al., 2018). Nuisance flooding occurs in Honolulu when the water level exceeds a certain threshold. Extreme events are more likely to occur when anticyclonic eddy-like anomalies are present during already high sea level due to signals from daily, seasonal, and decadal contributions (Firing & Merrifield, 2004). These extreme events are brought on when mesoscale eddy formation coincides with high periods in both annual and decadal cycles. The authors of Firing & Merrifield (2004), Caccamise et al. (2005), and Firing et al. (2005) agreed on the presence of an interdecadal oscillation signal. There is a long-term increasing trend in occurrences of these extreme sea level events which are attributed to sea level rise. Extreme sea level events can last from days to weeks; more concerning though is the intervals between their occurrences have decreased from 20+ years to approximately 5 years with sea level rise (Firing & Merrifield, 2004). During extreme sea level events, there have been reports of beach erosion, salt water inundation of fresh water aquifers, and flooding events in low-elevation areas not along a coastline (Firing & Merrifield, 2004). Although the extreme sea level events are somewhat

isolated instances at present, with sea level rising in Honolulu at a rate of 1.4 ± 0.3 mm/year (Caccamise et al., 2005), these events will become more common.

Chapter 2. Methods

2.1 Data

The data used in this study are gathered from a tide gauge in Honolulu and from satellite altimetry. These sources are complementary datasets and are useful in combination to help identify extreme sea level events and determine the dominant contributions to sea level variability in Hawai‘i. The effects of nuisance flooding caused by high sea level will be identified through photographs in the King Tides database.

2.1.1 Honolulu tide gauge data

Relative sea level observations are measured using an instrument called a tide gauge. The tide gauge used in this study is at the National Oceanic and Atmospheric Administration (NOAA) Station 1612340 located in Honolulu, HI. The sea level record for this location was established on January 1, 1905 and spans 113 years of continuous measurements, which makes it one the longest and highest-quality tide gauge records in the world. Currently, measurements are taken every 6 minutes. Hourly and daily data are made available for use by the University of Hawai‘i Sea Level Center (UHSLC). The type of tide gauge implemented at this station uses an acoustic sensor to measure sea level relative to a *benchmark*, or a fixed point on land. The sensor sends out packets of information as acoustic pulses down to the sea surface. The pulses are then reflected back to the sensor, and any phase changes that occur are recorded. Other types of tide gauges can also use pressure or radar sensors to complete their measurements. These instruments are capable of capturing signals from oceanographic variabilities such as tides, tsunamis, decadal climate oscillations, and swells. The data collected by tide gauges are also used as a method of comparison to ensure ocean models and satellite altimetry are not erroneous

in their own measurements. Tide gauges provide superior temporal resolution compared to satellite altimetry, as the length of gauge records can often exceed 100 years with each measurement taken minutes apart. Additionally, altimeters do not perform well with 50-100 km proximity to coastlines, but tide gauges are often installed right at the coastline and can sample the water directly. This makes tidal measurements essential when studying higher frequency coastal phenomenon that cannot be resolved using satellite altimetry methods. The main shortcoming of tide gauge observations is that they are limited to measurements relative to a benchmark. Since land motion can occur for a number of reasons on various time scales, it is vital to be identified and corrected for before any analysis of tide gauge observations can take place (Hamlington et al., 2016).

2.1.2 Satellite altimetry data

While tide gauges are useful for their high temporal resolution, the satellite altimeter data superiorly resolves spatial complexities. The accuracy achieved by the altimeters is on the order of centimeters. The current active satellite, Jason-3, records measurements at 3.3 cm precision with a goal of reaching 2.5 cm precision, but the errors are approximately normally distributed, and averaging these measurements over larger spatial areas allows for detection of even smaller variations. The spatial domain covers ±66° of latitude in ice-free oceans. Data made available from nearly continuous measurements from the TOPEX/Poseidon and Jason series satellite radar altimeters begin in October 1992 and span to present day. Measurements are taken with each full orbit of a satellite, which takes approximately 10 days to complete. The comparatively short record length of the altimetry data is not sufficient to generalize findings and requires tide gauges to provide long-term context. The temporal limitations in both the length of the altimetry

record and the interval between measurements require supplemental information from tide gauge data (Nerem & National Center for Atmospheric Research Staff (Eds), 2016). Since altimeters are capable of capturing detailed and expansive spatial information, satellite altimetry is useful in determining if sea level anomalies may be due to internal Rossby waves or eddies—phenomena undiscernible by tide gauges.

The altimetry data used in this study is provided by the Copernicus Marine Environment Monitoring Service (CMEMS). The CMEMS data is a gridded product and gives the time, longitude, and latitude of recorded sea level anomaly in millimeters. The spatial resolution of each grid is 0.25º latitude by 0.25º longitude, and the temporal resolution is daily average. Because the satellites only capture measurements once every 10 days, the values between each recording are interpolated to produce continuous daily data. For this study, the data from the beginning of 1993 through June 2018 was downloaded. In order to make a direct comparison between the altimetry data and the tide gauge data during this period, the long-term mean from the tide gauge data is removed from the altimetry data.

2.1.3 Sea level pressure data

Inclusion of sea level pressure (SLP) data is necessary to account for the minor contribution of the inverted-barometer effect to sea level. Measurement of SLP comes from the National Centers for Environmental Prediction (NCEP) and the National Center for Atmospheric Research (NCAR) Reanalysis Project, which began in 1991 (Kalnay et al., 1996). This dataset includes four-times daily global fields of SLP from 1948 to present on a 2.5º latitude-longitude grid. The closest grid cell to Honolulu was used to create a time series of SLP and estimate the inverted barometer effect in the following analysis.

2.1.4 Climate indices

Interannual to decadal modes of climate variability have been shown to affect coastal sea level across the Pacific as described in section 1.2.4 A monthly index of PDO state and PNA state were both made available by NOAA's National Centers for Environmental Information (NCEI). The correlation between the two indices will be determined. A comparison between the trend of these indices and the overall sea level trend will be made to determine if the anomalous observations of sea level in 2017 can be attributed to modes of climate variability.

2.1.4 King Tides database

The University of Hawai‘i Sea Grant College Program's Hawai‘i and Pacific Islands King Tides Project uses photos of areas affected by sea level extremes taken by volunteers in the Hawai‘i community (called 'citizen scientists') to build a database with the time, date, location, and descriptive information recorded for each photo. There is currently no data on physical components associated with the impacts recorded by the King Tides Project, which is a primary motivation of this work. This study will focus on Mapunapuna because it is an inland area impacted solely by sea level and does not need to consider waves.

2.2 Data analysis

2.2.1 Tidal analysis

The tide gauge sea level data is provided in referenced to a specific tidal datum: mean lower low water (MLLW). The MLLW is defined as the average of the lowest water level recorded per day over a specified epoch in a particular area. The area to be considered in this study is Honolulu Harbor, and the epoch used is known as the National Tidal Datum

Epoch (NTDE) as is determined by NOAA. The NTDE is defined as the time period from January 1, 1983 to December 31, 2001 and was chosen at such a length because it represents the nearest full-year count of the lunar nodal cycle (18.6 years). Using the tide gauge data, the MLLW was calculated by taking the average of the daily tidal minimums over the NTDE. Subtracting the MLLW from the tidal observations is often used as a standard reference level for the tide gauge observations.

Conversely, mean higher high water (MHHW) is a datum used to describe the average of the highest water level recorded per day over the same epoch, the NTDE. Using the MHHW is easier for some to understand in context, as it describes the average of the maximum sea level we should expect to observe. When true observations show measurements beyond the MHHW, the magnitude of high sea level events are more clearly illustrated. In this study, the products of the tidal analyses will be reported using the MHHW datum as it will make the final results easier to understand in context.

The software *UTide* allows users to generate tidal predictions given a set of time series observations (Codiga, 2017). By feeding the tides observed during the NTDE into this software, a tide prediction is made over the NTDE period. To create this prediction, UTide provides a group of constituents selected because of their contributions to tides (the principal lunar semidiurnal constituent, M_2, and the principal solar semidiurnal constituent, S_2, for example) and a confidence interval estimation for the tide gauge time series. This prediction can then be extrapolated forward and backward in time. Removing this prediction from the observed data, a residual signal is produced. Represented in this residual signal are the non-tidal contributors to sea level, such as secular trends, eddies, planetary waves, and the inverted barometer effect.

Tsunamis are also present, and because they are severe and atypical sea level events unrelated to tides or climate indices, they can cause a malformed tide prediction to be created and should thus be removed from the data. The most significant tsunami events were identified by their large trademark ‘ringing’ signal in the tidal residuals, and the dates on which they occur were removed from the original data set before generating a second and final tidal prediction as described above. The following tsunami events were identified and removed from the tide gauge data: November 4-10, 1952; May 23-25, 1960; March 28 to April 3, 1964; February 27 to March 2, 2010; March 11-15, 2011. News articles reporting tsunamis on each of these dates can be found, corroborating the events did indeed occur.

2.2.2 Convolution filters

A convolution filter incrementally applies a filter shape to a dataset, taking a predetermined range of data and smoothing it by taking a weighted average of the data within each increment. Convolution filters can be used in both time and space dimensions and will aid this analysis by distinguishing between the various contributions to Honolulu sea level at different time and space scales. For the tide gauge data, the filter will be applied in the temporal domain, and for the altimetry data, the filter will be applied in the spatial domain.

To assess the contribution of long-term trends and decadal climate modes on the recent record-high sea levels in Honolulu, the tide gauge data is smoothed by applying a convolution filter in the temporal domain with weights defined by windowed cardinal sine (abbreviated *sinc*) function over the monthly averages of the series. By using a lowpass filter with a cutoff frequency of approximately 18 months, the filtering procedure isolates

the interannual and longer variability in the observations. This filter is also applied to the PDO and PNA signals for use in a multiple linear regression as discussed in the next section.

In the spatial domain, the large-scale and mesoscale energy bands in the satellite altimetry data are separated by applying a 2D Gaussian convolution filter using an appropriate scaling factor. The Rossby radius of deformation varies by latitude and determines the horizontal scale at which point rotation begins to influence ocean perturbations (Figure 6. The Rossby radii of deformation (from Chelton et al., 1998).). The Rossby radius of deformation, *r*, is defined as:

$$r = \frac{c}{f} = \frac{c}{|2\Omega \sin(\theta)|} \quad \text{if } |\theta| \gtrsim 5°$$

where *f* is the Coriolis parameter, Ω is the Earth's rate of rotation, and θ is latitude (Chelton et al., 1998). In Hawai'i, this value is ~60 km (Figure 6. The Rossby radii of deformation (from Chelton et al., 1998).). Twice the Rossby radius of deformation shall be used to

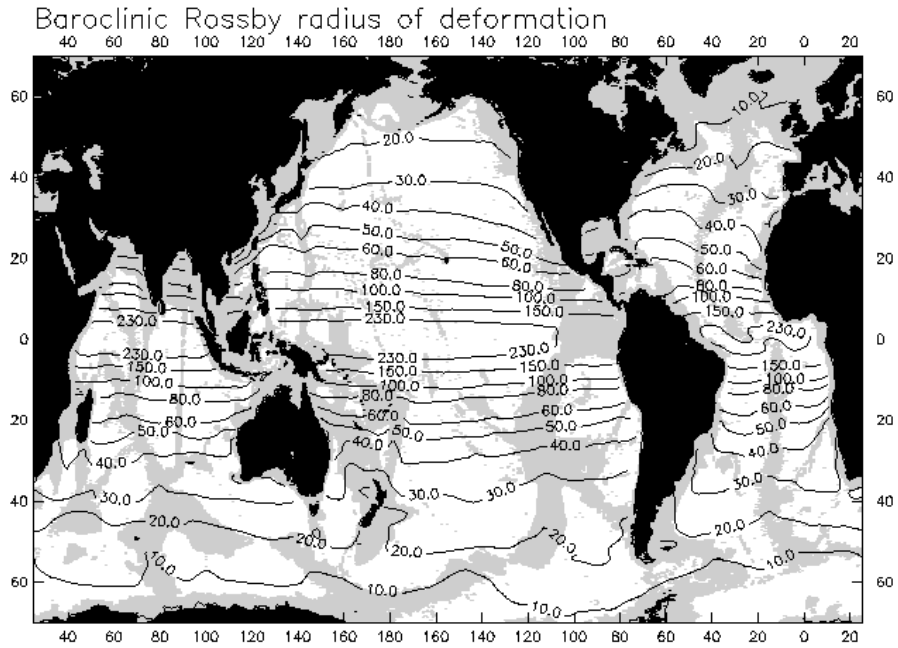

ensure that the largest scales are excluded from the mesoscale.

Figure 6. The Rossby radii of deformation (from Chelton et al., 1998).

After applying the filter based on the Rossby radius, the large-scale variability is considered to be dominated by Rossby waves, while the residual mesoscale variability is considered to be dominated by eddies. A region of the ocean around the Hawaiian archipelago is isolated from the global grid of the satellite altimetry data. Honolulu is located at 21° 18' N 157° 52' W, therefore the data included will be from 31º N to 11º N and from 177º W to 107 º W. In the days surrounding an extreme sea level event (as identified in the tide gauge data), the altimetry record grids will be examined in this boxed area to determine the relative contributions of eddies and Rossby waves to the event. A time series of eddy and Rossby wave activity is extracted at the altimetry point nearest to the Honolulu tide gauge location.

2.2.3 Least-squares multiple linear regression

Multiple linear regression (MLR) is a technique used to find an optimally weighted linear combination of multiple predictors that account for fractions of variability in a time series or dataset. The 'least squares' version of MLR provides a solution which minimizes the sum of the squares of the residuals, or in this case, the differences between the observed sea level and the predicted sea level. Here, MLR analysis will be applied to sea level data from the Honolulu tide gauge to simultaneously estimate the long-term trend, the annual and semiannual harmonics, and the contribution to sea level variability from two modes of decadal climate variability: The Pacific Decadal Oscillation (PDO) and the Pacific North American (PNA) pattern.

In addition to the climate indices themselves, the Hilbert transform of the PDO and the PNA are also included in the MLR. The Hilbert transform works by first processing an original signal into frequency components via the Fourier transform. Each Fourier

component then undergoes a 90^{o} phase shift before being back-transformed into the time domain to complete the Hilbert transform. The purpose of including the Hilbert transform of each index in the MLR is to capture the potential for phase lag between variability in the index and the response of the sea level to the climate mode in Honolulu. The total contribution of a climate mode to sea level is calculated as the sum of the index and its Hilbert transform multiplied by the respective regression coefficients. It is also important to note that the PDO and PNA are not significantly correlated ($r < 0.3$) over the period of the regression, suggesting that it is possible to statistically distinguish the variability owing to each individual mode.

2.3 Oceanographic metadata for King Tides database

When sea level conditions are met for nuisance flooding to occur as found in the tide gauge and satellite altimetry data, the King Tides database is searched using the time and location of these flagged events. The photographs associated with these events are collected, and a visual representation of the effects of nuisance flooding are made available. In this study, I will relate this metadata to physical conditions in Honolulu, which will improve understanding of how future events may impact the area. Applying the quantified physical information to the King Tides database will provide a better understanding of how high tides, ocean dynamics, and extreme sea level events affect an area. This can then be used to forecast expected conditions when similar events are predicted to occur in the future, with special consideration for the continuing threat of sea level rise.

Chapter 3. Results

3.1 History of Nuisance flooding in Honolulu

The threshold for nuisance flooding in Honolulu is approximately 32 cm above MHHW. Using the tide gauge record from Honolulu Harbor, the number of days per year experiencing nuisance flooding events were calculated between 1905 and 2018 (Figure 7. Counts of nuisance flooding events over the tide gauge time series). Nuisance flooding events did not appear in the record until 1964, where 3 occurred in that year. Prior to 2017, the yearly flooding events ranged between 0 and 5, and the maximum number of events occurred in 1984, 1995, and 2003, each tied at 5 events per year. In 2017, 15 events were recorded, which is a record three times greater than the previous ones.

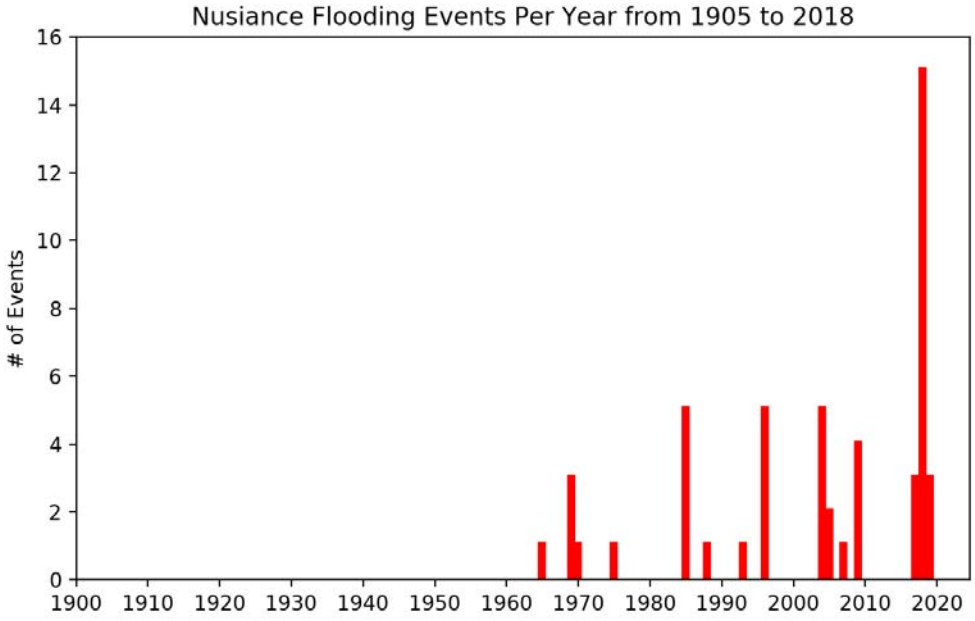

Figure 7. Counts of nuisance flooding events over the tide gauge time series.

3.2 Observations and impacts during 2017

During the record-setting summer of 2017, the King Tides database documented the impacts of the nuisance flooding due to the high sea levels. The Mapunapuna area is an industrial area near the Honolulu airport that is particularly vulnerable to nuisance flooding due to its low elevation. The King Tides database contains photo documentation of impacts in Mapunapuna for the following seven dates in 2017: May 23, 25-27, June 23-24, and July 22 (Figure 8. Photos from the King Tides database for some Mapunapuna events in 2017. select dates).

For brevity, the focus of the following analysis will be on the contributions to the high sea levels on these seven dates for the Mapunapuna, but contributions for all dates and locations in the database can be calculated using the following techniques. In addition to the dates in the King Tides database, the dynamics on April 29, 2017 and August 21, 2017 will also be considered, as these dates experienced the most extreme sea levels despite not being photo-documented, and these dates are important for demonstrating the variance in the relative importance of the dynamic contributions.

The daily maximum sea levels recorded from the tide gauge data were found for each of the aforementioned dates (Table 1, Figure 14: 'TG-SL'), and the purpose of the following analysis is to identify the process contributions to these anomalies. The largest tide gauge observations found in each month from April to August 2017 that meet the qualification for a nuisance flooding event were identified and noted (Figure 9. Nuisance flooding threshold shown as black dashed line. Nuisance flooding events shown as orange circles on 04-29-2017, 05-27-2017, 06-24-2017 and 08-21-2017, respectively.). It is important to note that the dates May 23, 2017, May 25, 2017, and July 22, 2017 were

included in the King Tides database but were not found to cross the nuisance flooding threshold (Table 1; Figure 14). Nuisance flooding by definition causes inconveniences to the public (see Preface), so although there may be photographs that depict water in the streets, it may not have been an amount significant enough to prevent access to cars and pedestrians. Although not in the King Tides database for the Mapunapuna area, the following two dates were considerably important to note and therefore included in this analysis: April 29, 2017 broke the daily average sea level record in for the Honolulu tide gauge at 23.951 cm, and August 21, 2017 broke the daily maximum sea level record over the entire tide gauge time series at 42.169 cm (Table 1; Figure 14; Figure 9. Nuisance flooding threshold shown as black dashed line. Nuisance flooding events shown as orange circles on 04-29-2017, 05-27-2017, 06-24-2017 and 08-21-2017, respectively.). As mentioned in Section 2.2.1, the data are standardized to MHHW; therefore, MHHW is located at 0 cm in all reported result (Figure 10. Red dashed lines indicate MHHW (top) and MLLW (bottom).).

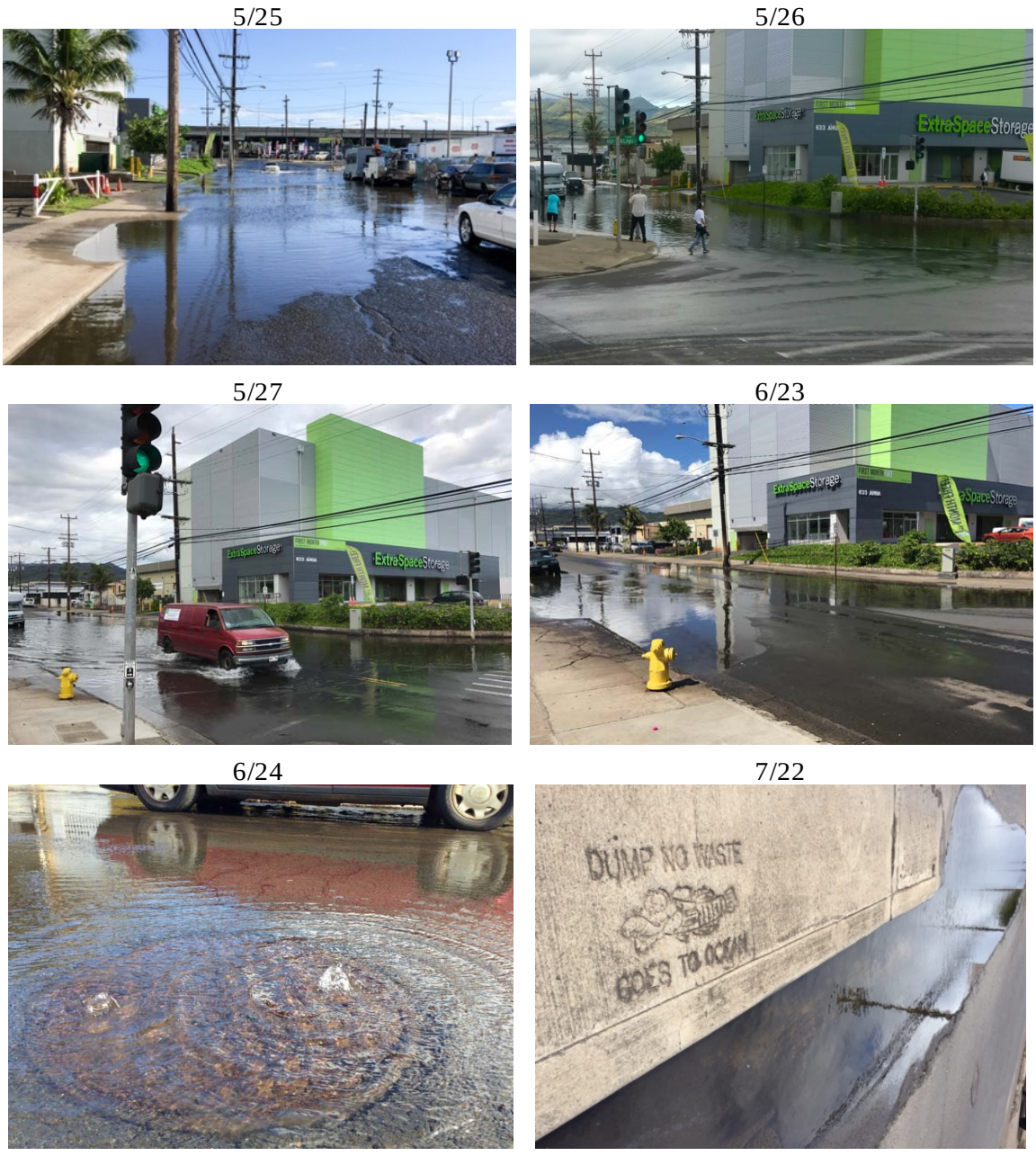

Figure 8. Photos from the King Tides database for some Mapunapuna events in 2017.

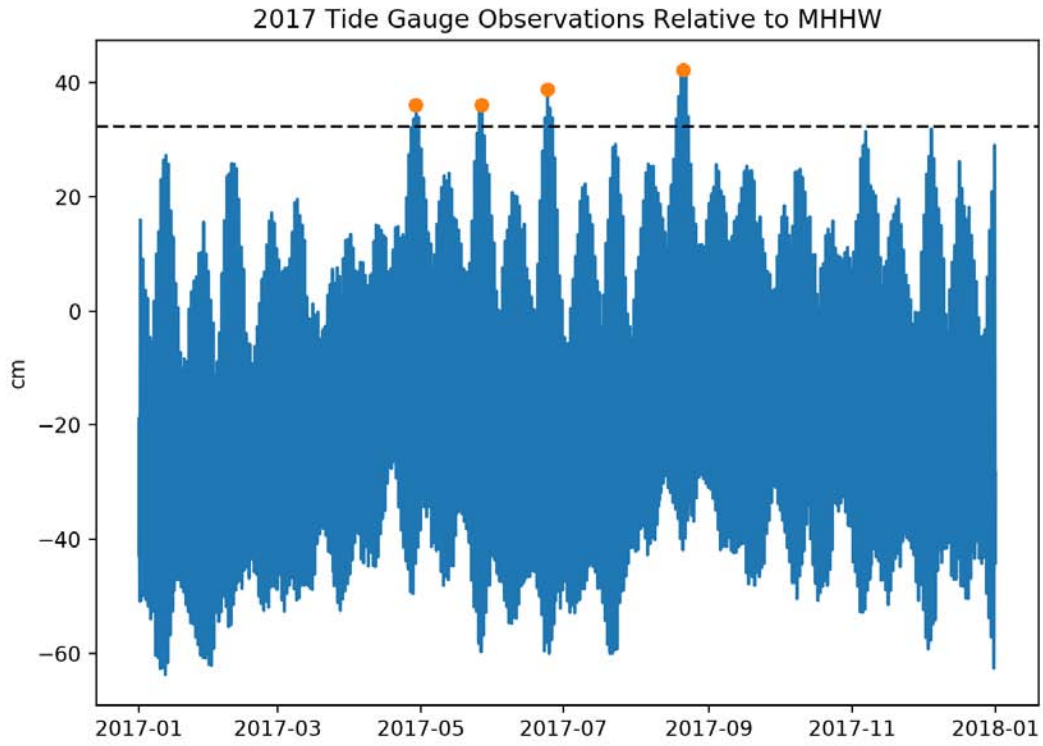

Figure 9. Nuisance flooding threshold shown as black dashed line. Nuisance flooding events shown as orange circles on 04-29-2017, 05-27-2017, 06-24-2017 and 08-21-2017, respectively.

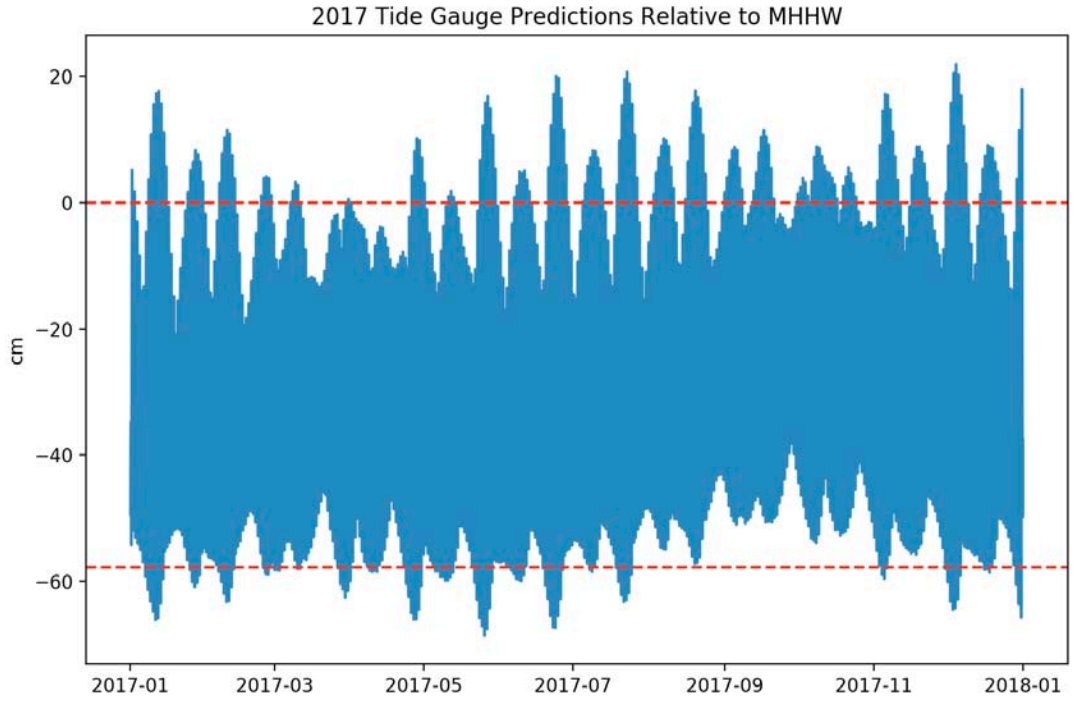

Figure 10. Red dashed lines indicate MHHW (top) and MLLW (bottom).

3.3 Contributions to high sea level events

The stacking of sea level comes from the various contributions which sum to the observed sea level (Figure 14). The maximum observed sea level is made up of the following contributions which may or may not have combined with one another to lead to a nuisance flooding event. The stacking of these elements is simulated in Figure 14.

3.3.1 Sea level rise

The amount of sea level rise from 1905 to 2017 has been a total of 15.7 cm. The amount of sea level rise from 1992 to 2017 has been 3.5 cm.

3.3.2 Interannual to decadal contributions

To isolate the lowest-frequency contributions, the sinc function was applied to the tide gauge, PDO, and PNA sea level data from 1993 to 2018 using methods described in Section 2.2.3. Using the lowpass filtered PDO, PNA, their Hilbert transforms, and tide gauge data, a least-squares regression was performed to determine the PDO and PNA contributions to the tide gauge signal. Once the high frequency signal was removed, the remaining signal shows the low frequency component, which is effectively the contribution to sea level excluding time scales greater than annual or semiannual in occurrence. The correlation between the PDO and PNA was low ($r \approx 0.3$). Figure 11. Interdecadal contributions to the filtered tide gauge sea level from 1993 to 2018. shows the relative contributions of the climate indices against the tide gauge signal. It is evident that the anomalous sea level trend in 2017 had little it could attribute to modes of climate variability (Figure 11. Interdecadal contributions to the filtered tide gauge sea level from 1993 to 2018.).

3.3.3 Identifying contributions from Rossby waves and eddies

A 2D Gaussian convolution filter was applied to the altimetry data as described in Section 2.2.3, separating the large-scale contributions from the eddy-scale contributions. I removed the long-term mean (1993 to June 2018) from the altimetry data. In order to make the tide gauge time series and the altimetry data comparable, I leveled the two by removing the tide gauge long-term mean from the altimetry data, affecting the altimetry sea level anomaly (Table 1, Figure 14: 'ALT-SLA'), the Rossby wave, or planetary scale, contribution (Table 1, Figure 14: 'ROSSBY'), and the eddy, or mesoscale, contribution (Table 1, Figure 14: 'EDDY'). The Rossby wave contributions varied between each event, ranging from 7.712 cm to 13.944 cm (Table 1; Figure 13. Comparison between dates of planetary scale anomalies, such as Rossby waves, and mesoscale anomalies, such as eddies, near Hawaii.; Figure 14). On August 21, 2017, the greatest contribution from Rossby waves of all events occurred, with a value of 13.944 cm (Table 1; Figure 12. Planetary scale and mesoscale sea level anomalies around the Hawaiian archipelago.; Figure 14). The values for the eddy contributions were not constant and varied widely between each event, ranging from -3.807 cm to 8.685 cm (Table 1; Figure 13. Comparison between dates of planetary scale anomalies, such as Rossby waves, and mesoscale anomalies, such as eddies, near Hawaii.; Figure 14). The greatest contribution from eddies occurred on April 29, 2017, with a value of 8.685 cm.

3.3.4 Inverted-barometer contribution

The overall contributions from the inverted-barometer effect were minimal in most instances of the time series, ordering on the magnitude of millimeters. The values ranged from -1.399 cm to 4.301 cm (Table 1, Figure 14: 'IB-SL'). Of all the events, the greatest

contribution from the inverted-barometer effect came on April 29, 2017 with a value of 4.301 cm.

3.3.5 Tidal variability

The typical daily tidal range, given by the difference between MHHW and MLLW, was 57.665 cm, but this range was substantially exceeded on some of the days examined here (Figure 10. Red dashed lines indicate MHHW (top) and MLLW (bottom).). The maximum predicted tidal contribution for each event ranged from -1.315 cm on May 23, 2017 to 20.054 cm on June 24, 2017 (Table 1, Figure 14: 'PR-TD'; Figure 10. Red dashed lines indicate MHHW (top) and MLLW (bottom).). The difference in sea level between the predicted tide and the observed tide were averaged by day and reported as the residual sea level (Table 1, Figure 14: 'TG-RSL'). The contribution from Rossby waves, eddies, and the inverted barometer effect are all echoed in this residual value.

cm (relative to MHHW)

Figure 11. Interdecadal contributions to the filtered tide gauge sea level from 1993 to 2018.

Figure 12. Planetary scale and mesoscale sea level anomalies around the Hawaiian archipelago.

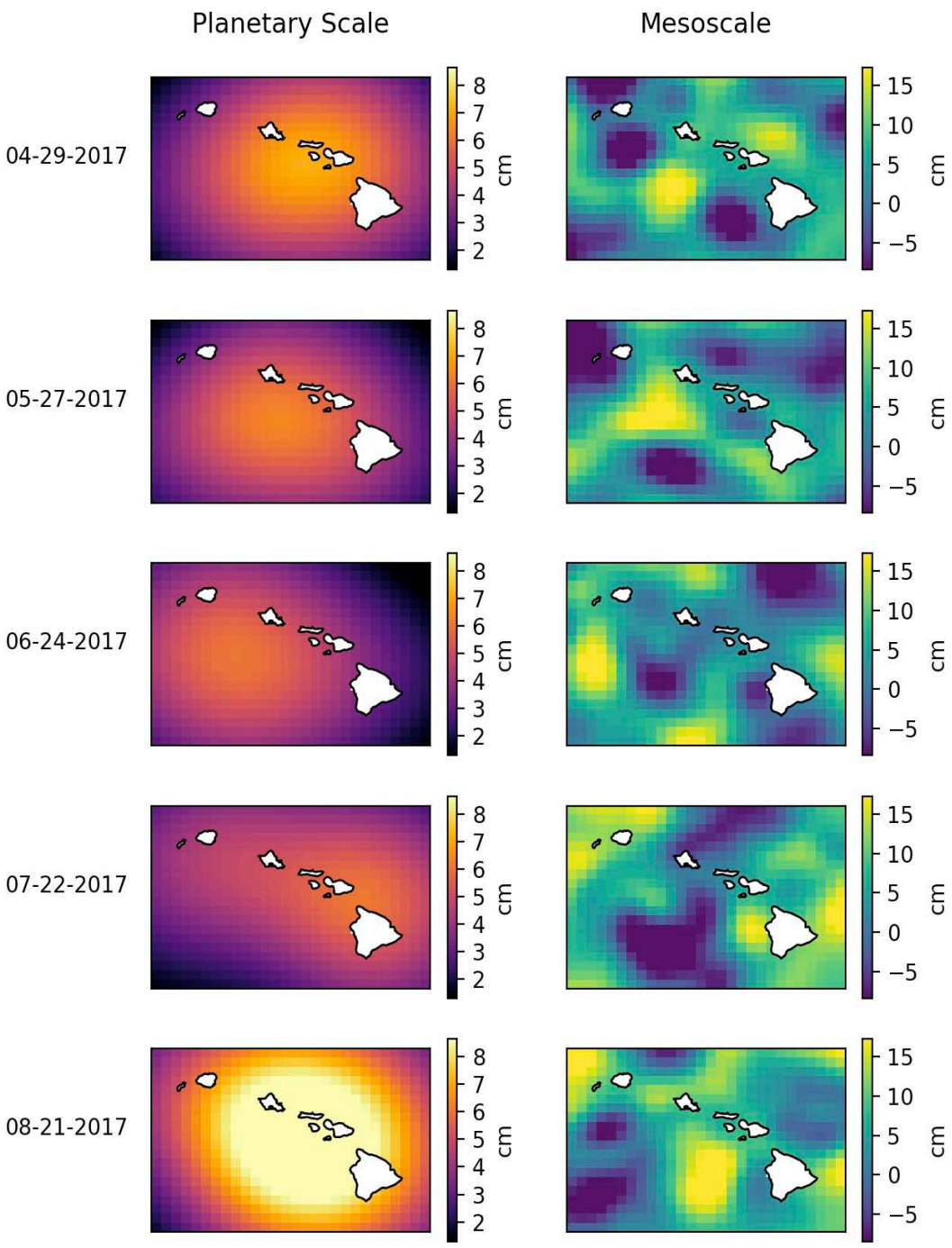

Figure 13. Comparison between dates of planetary scale anomalies, such as Rossby waves, and mesoscale anomalies, such as eddies, near Hawaii.

Table 2. All values in cm relative to MHHW. Daily Max: the daily maximum observed sea level (TG-SL) and predicted tides (PR-TD) from tide gauge data. Daily Averaged Sea Level: the daily averaged contributions to sea level from the tide gauge-derived residual (TG-RSL), the altimetry-derived sea level anomaly (ALT-SLA), the large-scale sea level component from the altimetry (ROSSBY), the eddy-scale sea level component from the altimetry (EDDY), and the inverted-barometer sea level (IB-SL).

	Daily Max (cm)		Daily Averaged Sea Level (cm)				
	TG-SL	PR-TD	TG-RSL	ALT-SLA	ROSSBY	EDDY	IB-SL
4/29/17	36.169*	9.839	23.951	17.461	8.777	8.685	4.301
5/23/17	15.769	-1.315	16.814	16.521	9.170	7.351	-1.399
5/25/17	31.169	12.200	14.615	14.881	9.038	5.844	-1.274
5/26/17	35.969*	15.808	13.747	13.511	8.938	4.573	0.051
5/27/17	36.169*	16.886	13.184	12.561	8.864	3.697	0.926
6/23/17	33.869*	17.219	12.375	7.181	7.791	-0.610	1.926
6/24/17	38.869*	20.054	11.305	7.011	7.712	-0.701	1.376
7/22/17	28.669	19.487	6.109	4.271	8.079	-3.807	0.701
8/21/17	42.169*	16.693	22.236	18.191	13.944	4.247	0.876

** indicates nuisance flooding occurs (TG-SL > 32 cm).*

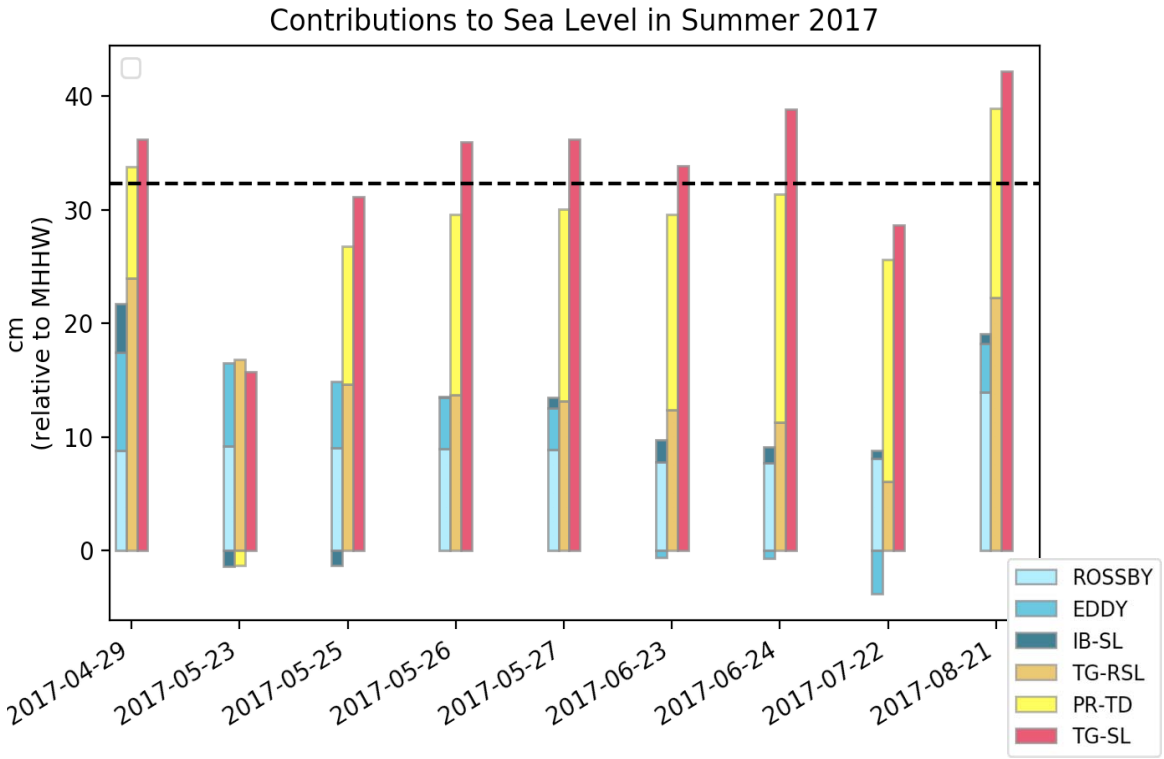

Figure 14. Various contributions to nuisance flooding events on flagged dates in 2017 (values and abbreviations correspond to those in Table 1). Dashed line represents the nuisance flooding threshold.

3.4 Nuisance flooding events

3.4.1 April 29, 2017

When the predicted tide is high (generally during a spring tide), it becomes easier for sea level to cross the threshold into a nuisance flooding event. This was not the case on April 29, 2017. This date is exceptional because of its qualification as a nuisance flooding event even with a relatively low tidal contribution when compared to other events. On this day, the daily maximum sea level was found to be 36.169 cm, but the contribution from tides on this day was merely 9.839 cm. On other days when nuisance flooding occurred, the contribution from the predicted tide was higher by 6 cm or more (see Table 1, Figure 14). Using May 27, 2018 as an example, the predicted tide was 16.886 cm producing with other contributors a maximum sea level of 36.169 cm. Even though the tidal prediction was 6.897 cm less on April 29, the maximum sea levels were identical to one another on the two dates.

The contributions from Rossby waves, eddies, and the inverted-barometer effect on April 29 were among the highest of all the events identified. Rossby waves contributed 8.777 cm of sea level, eddies contributed 8.685 cm, and the inverted-barometer effect contributed another 4.301 cm. The total residual sea level of 23.951 cm exceeded all other days in the entire 2017 time series. Had the tides been higher on this date, it may have been a comparable event to the one observed on August 21, 2017, which broke the 112-year tide gauge record.

3.4.2 May 23 and May 25, 2017

Neither of the events on May 23 nor May 25, 2017 crossed the threshold into a flood event. The predicted tide on May 23 was -1.315 cm, which made it appear to be an

abnormal inclusion to the database because flooding events are typically forecasted to occur during high tide. The predicted tide on May 25 at 12.200 cm was possibly enough to lend itself to a flooding event, though one did not occur, as the total maximum sea level on this day was 31.169 cm. These dates were immediately followed by events that did cross the nuisance flooding threshold, so although these dates did not ultimately qualify as flood events, the inclusion of these dates in the King Tides database in anticipation flood events was reasonable. These dates also bring to light the possible errors that may arise when predicting flooding events. Another interesting thing to note is that the contribution from the inverted-barometer effect was negative on both of these days, unlike any of the other events in this study, which may have contributed against a flooding event.

3.4.3 May 26 and May 27, 2017

The events on May 26 and May 27, 2017 were comparable in magnitude to one another, varying by about a centimeter or less in all contribution categories. The maximum sea level on May 26 was 35.969 cm and on May 27 was 36.869 cm. Both of these events crossed the nuisance flooding threshold. The tides on these days were predicted to be high: 15.808 cm on May 26 and 16.886 cm on May 27. Contribution from Rossby waves was 8.938 cm on May 26 and 8.864 cm on May 27. Contribution from eddies was 4.573 cm on May 26 and 3.697 cm on May 27. Contribution from the inverted-barometer effect were less than a centimeter on both days.

3.4.4 June 23 and June 24, 2017

Both the events on June 23 and June 24 crossed the nuisance flooding threshold. The maximum sea level observed on June 23 was 33.869 cm, which was 5 cm less than it was on June 24, which had a value of 38.869 cm, though the events were only 24 hours

apart. The primary reason for this discrepancy is found in the predicted tides for each day. On June 23, the predicted tide was 17.219 cm, whereas on June 24 the predicted tide was at 20.054 cm. Contributions from all other sources differed by less than 1 cm between the two dates.

3.4.5 July 22, 2017

July 22 did not qualify as a nuisance flooding event, despite high tides. The residual sea level on this day was merely 6.109 cm. The contribution from Rossby waves 8.079 cm. The eddy contribution was -3.807 cm, which was likely a key factor in reducing the residual and the absence of a flooding event. The inverted-barometer effect contributed less than a centimeter of sea level.

3.4.6 August 21, 2017

The sea level on August 21 broke the 112-year tide gauge record at 42.169 cm. The tidal prediction for this date was 16.693 cm. The residual sea level on this day was 22.236 cm. The contribution from Rossby waves was the greatest of all the flagged events on this date, measured at 13.944 cm. Eddies contributed another 4.247 cm, and the inverted-barometer effect contributed less than 1 cm. The magnitude of this record-breaking event is best illustrated when compared to other events observed in the time series. The sea level during Hawai‘i’s most devastating hurricane in recent history, Hurricane Iniki, was at a maximum on September 12, 1992, when it reached 40.669 cm. The maximum sea level on August 21, 2017 exceeded the sea level during Hurricane Iniki by about 2 cm.

Chapter 4. Summary and Discussion

4.1 Contributions to sea level

The daily means from the tide gauge data and the altimetry data differed for each of the events in Table 1. Ideally these numbers would be identical, but differences in the methodology by which the data are collected lead to a disagreement in the final values (Figure 14). As mentioned in sections 2.1.1 and 2.1.2, the Honolulu tide gauge takes in situ measurements with hourly sampling intervals, but the altimeters can only obtain measurements once every 10 days. The data provided between altimetry measurements are interpolated values by necessity and may not be as accurate as direct measurements. Although the altimetry measurements themselves may not be accurate, the ability to see the spatial structure is highly valuable as this is unobtainable information from tide gauge measurements alone. Knowing the relative contributions from Rossby waves or eddies is important when making sea level estimations. It did not appear that the April 29, 2017 nuisance flooding event was expected to occur by the King Tides Project. This was likely because the contribution from tides was not estimated to be high, therefore no event was anticipated. The contribution from eddies on this day proved to be significant. This event highlights the nonnegligible role Rossby waves and eddies may play in the computation of sea level beyond the consideration of predicted tides alone. The inverted barometer effect was generally less than a centimeter in magnitude, so as speculated in Section 1.2.8, their contribution to sea level were minimal. Consideration of these ocean phenomena in addition to tidal predictions are valuable when making estimates of when nuisance flooding events may occur. The contribution from the predicted tide is a primary indicator for when a nuisance flooding event may appear, though its occurrence cannot be guaranteed. This

was just the case on July 22, 2017, when the predicted tide was >19 cm, but no flooding event occurred. As sea level continues to rise as the ice sheets melt and the ocean undergoes thermal expansion, these nuisance flooding events can be expected to occur more frequently.

4.2 Unaccounted contributions to sea level

Ideally, the residual sea level would be equal to the sum of the altimetry components from Rossby waves and eddies and the inverted barometer effect; however, this was not necessarily true (Figure 14). The explanation for this disagreement may be found in unaccounted contributions to the sea level. The following factors are all important to consider but are beyond the scope of this study. Harbor resonance can cause an apparent increase in sea level when oscillations within a harbor are amplified at their natural frequencies (Dong et al., 2010). Coastal trapped waves are considered a mixture of Kelvin waves and continental shelf waves and can cause local changes to sea level (Wang & Mooers, 1976). Because the methods used to create the tidal prediction are not perfect, there may be some minor dissonance between the predicted tides and the observed tides which have not been adjusted for in this study.

4.3 King Tides Project

The physical components found in this study would be an excellent supplement to the already impressive King Tides database and would further the understanding of these anomalous events. The model created in this study can serve as a prototype for a product with expanded knowledge.

4.4 Future work

Using Mapunapuna as the study area allowed for the influence of waves to be ignored because of its inland geography. In future studies, the additional consideration of this component would expand the application to coastal areas. Because satellite altimetry requires interpolated data, there is some concern with its use around islands like those found in Hawai‘i. This issue would need to be addressed in subsequent work.

References

Caccamise, D. J., Merrifield, M. A., Bevis, M., Foster, J., Firing, Y. L., Schenewerk, M. S., … Thomas, D. A. (2005). Sea level rise at Honolulu and Hilo, Hawaii: GPS estimates of differential land motion. *Geophysical Research Letters*, *32*(3), 1–4. https://doi.org/10.1029/2004GL021380

Chelton, D. B., deSzoeke, R. A., Schlax, M. G., El Naggar, K., & Siwertz, N. (1998). Geographical Variability of the First Baroclinic Rossby Radius of Deformation. *Journal of Physical Oceanography*, *28*(3), 433–460. https://doi.org/10.1175/1520-0485(1998)028<0433:GVOTFB>2.0.CO;2

Chelton, D. B., & Schlax, M. G. (1996). Global Observations of Oceanic Rossby Waves. *Science*, *272*(5259), 234–238. https://doi.org/10.1126/science.272.5259.234

Church, J. A., Clark, P. U., Cazenave, A., Gregory, J., Jevrejeva, S., Levermann, A., … Unnikrishnan, A. S. (2013). Sea level change. In Intergovernmental Panel on Climate Change (Ed.), *Climate Change 2013: The Physical Science Basis. Contribution of Working Group I to the Fifth Assessment Report of the Intergovernmental Panel on Climate Change* (pp. 1137–1216). Cambridge: Cambridge University Press. https://doi.org/10.1017/CB09781107415315.026

Church, J. A., Woodworth, P. L., Aarup, T., & Wilson, W. S. (2010). *Understanding Sea-Level Rise and Variability*. *Wiley-Blackwell*. https://doi.org/10.1002/9781444323276

Cocke, S. (2015). Waikiki Beach Is Totally Man-Made (And Disappearing). Can Hawaii Save It? *HuffingtonPost.Com*. Retrieved from http://www.huffingtonpost.com/2015/03/09/saving-waikiki-beach-erosion_n_6835424.html

Codiga, D. (2017). *Unified Tidal Analysis and Prediction Using the UTide Matlab Functions*. Narragansett, RI. Retrieved from ftp://www.po.gso.uri.edu/ pub/downloads/codiga/pubs/2011Codiga-UTide-Report.pdf

DeConto, R. M., & Pollard, D. (2016). Contribution of Antarctica to past and future sea-level rise. *Nature*, *531*(7596), 591–597. https://doi.org/10.1038/nature17145

Department of Business Economic Development & Tourism. (n.d.). Research & Economic Analysis. Retrieved November 6, 2018, from http://dbedt.hawaii.gov/

Dong, G., Wang, G., Ma, X., & Ma, Y. (2010). Harbor resonance induced by subaerial landslide-generated impact waves. *Ocean Engineering*, *37*(10), 927–934. https://doi.org/10.1016/j.oceaneng.2010.03.005

Firing, Y. L., & Merrifield, M. A. (2004). Extreme sea level events at Hawaii: Influence of mesoscale eddies. *Geophysical Research Letters*, *31*(24), 1–4. https://doi.org/10.1029/2004GL021539

Firing, Y. L., Merrifield, M. A., Schroeder, T. A., & Qiu, B. (2005). Interdecadal sea level fluctuations at Hawaii. *Bulletin of the American Meteorological Society*, *86*(1), 32–33. https://doi.org/10.1175/JPO2636.1

Gornitz, V. (2012). The Great Ice Meltdown and Rising Seas: Lessons for Tomorrow. Retrieved from https://www.giss.nasa.gov/research/briefs/gornitz_10/

Haigh, I. D., Eliot, M., & Pattiaratchi, C. (2011). Global influences of the 18.61 year nodal cycle and 8.85 year cycle of lunar perigee on high tidal levels. *Journal of Geophysical Research: Oceans*, *116*(6), 1–16. https://doi.org/10.1029/2010JC006645

Hamlington, B. D., Thompson, P. R., & National Center for Atmospheric Research Staff (Eds). (2016). The Climate Data Guide: Tide gauge sea level data. Retrieved from https://climatedataguide.ucar.edu/climate-data/tide-gauge-sea-level-data

Hawai‘i Climate Change Mitigation and Adaptation Commission. (2017). Hawai‘i Sea Level Rise Vulnerability and Adaptation Report. *Prepared by Tetra Tech, Inc. and the State of Hawai‘i Department of Land and Natural Resources, Office of Conservation and Coastal Lands, under the State*

of Hawai'i Department of Land and Natural Resources Contract No: 64064.

Hays, J. D., Imbrie, J., & Shackleton, N. J. (1976). Variations in the Earth's Orbit: Pacemaker of the Ice Ages. *Science*, *194*(4270), 1121–1132. https://doi.org/10.1126/science.194.4270.1121

Kalnay, E., Kanamitsu, M., Kistler, R., Collins, W., Deaven, D., Gandin, L., … Joseph, D. (1996). The NCEP/NCAR 40-Year Reanalysis Project. *Bulletin of the American Meteorological Society*, *77*(3), 437–471. https://doi.org/10.1175/1520-0477(1996)077<0437:TNYRP>2.0.CO;2

Lumpkin, R., & Flament, P. (2001). Lagrangian statistics in the central North Pacific. *Journal of Marine Systems*, *29*(1–4), 141–155. https://doi.org/10.1016/S0924-7963(01)00014-8

Mantua, N. J., Hare, S. R., Zhang, Y., Wallace, J. M., & Francis, R. C. (1997). A Pacific Interdecadal Climate Oscillation with Impacts on Salmon Production. *Bulletin of the American Meteorological Society*, *78*(6), 1069–1079. https://doi.org/10.1175/1520-0477(1997)078<1069:APICOW>2.0.CO;2

Merrifield, M. A., Thompson, P. R., & Lander, M. (2012). Multidecadal sea level anomalies and trends in the western tropical Pacific. *Geophysical Research Letters*, *39*(13), 2–6. https://doi.org/10.1029/2012GL052032

Nerem, R. S., & National Center for Atmospheric Research Staff (Eds). (2016). The Climate Data Guide: Global Mean Sea Level from TOPEX & Jason Altimetry. Retrieved January 19, 2016, from https://climatedataguide.ucar.edu/climate-data/global-mean-sea-level-topex-jason-altimetry

NOAA. (2018). What is high tide flooding? Retrieved June 11, 2018, from https://oceanservice.noaa.gov/facts/nuisance-flooding.html

Sweet, W. V., Dusek, G., Obeysekera, J., & Marra, J. J. (2018). Patterns and Projections of High Tide Flooding Along the U. S. Coastline Using a Common Impact Threshold, (February), 56. Retrieved from https://tidesandcurrents.noaa.gov/publications/techrpt86_PaP_of_HTFlooding.pdf

Thompson, P. R., Merrifield, M. A., Wells, J. R., & Chang, C. M. (2014). Wind-driven coastal sea level variability in the northeast pacific. *Journal of Climate*, *27*(12), 4733–4751. https://doi.org/10.1175/JCLI-D-13-00225.1

Virtue, J. (2017, July). With King Tides, Experts Predict Rising Sea Levels to Continue. *Hawaii Business Magazine*. Retrieved from https://www.hawaiibusiness.com/with-king-tides-experts-predict-rising-sea-levels-to-continue/

Wallace, J. M., & Gutzler, D. S. (1981). Teleconnections in the Geopotential Height Field during the Northern Hemisphere Winter. *Monthly Weather Review*. https://doi.org/10.1175/1520-0493(1981)109<0784:TITGHF>2.0.CO;2

Wang, D.-P., & Mooers, C. N. K. (1976). Coastal-Trapped Waves in a Continuously Stratified Ocean. *Journal of Physical Oceanography*. https://doi.org/10.1175/1520-0485(1976)006<0853:CTWIAC>2.0.CO;2

Yoshida, S., Qiu, B., & Hacker, P. (2010). Wind-generated eddy characteristics in the lee of the island of Hawaii. *Journal of Geophysical Research: Oceans*, *115*(3), 1–15. https://doi.org/10.1029/2009JC005417